



# Isotopically exchangeable organic hydrogen in coal relates to thermal maturity and maceral composition

M. Mastalerz<sup>a,\*</sup>, A. Schimmelmann<sup>b</sup>

<sup>a</sup>*Indiana Geological Survey, Indiana University, 611 North Walnut Grove, Bloomington, IN 47405-2208, USA*

<sup>b</sup>*Department of Geological Sciences, Indiana University, Bloomington, IN 47405-1405, USA*

Received 6 November 2001; accepted 22 May 2002  
(returned to author for revision 15 March 2002)

## Abstract

Hydrogen isotopic exchangeability ( $H_{ex}$ ) and  $\delta D_n$  values of non-exchangeable organic hydrogen were investigated in coal kerogens ranging in rank from lignite to graphite. The relative abundance of  $H_{ex}$  is highest in lignite with about 18% of total hydrogen being exchangeable, and decreases to around 2.5% in coals with  $R_o$  of 1.7 to ca. 5.7%. At still higher rank ( $R_o > 6\%$ ),  $H_{ex}$  increases slightly, although the abundance of total hydrogen decreases.  $\delta D_n$  is influenced by original biochemical D/H ratios and by thermal maturation in contact with water. Therefore,  $\delta D_n$  does not show an overall consistent trend with maturity. © 2002 Elsevier Science Ltd. All rights reserved.

## 1. Introduction

Total organic hydrogen in coal encompasses hydrogen that is linked to carbon either directly or via bridging heteroatoms like O, S, and N. Some of this organic hydrogen can isotopically exchange with hydrogen from ambient water, with exchange half-lives ranging from seconds (in exposed hydroxyl, carboxyl, and amino groups) to millions of years (aliphatic carbon-linked hydrogen; Schimmelmann et al., 1999). The abundance of readily exchangeable organic hydrogen is expressed as “hydrogen exchangeability” ( $H_{ex}$ , in % of total organic hydrogen, measured after ca. 8 h of contact with deuterium-enriched water vapor at 115 °C; Schimmelmann et al., 1999). Exchangeable organic hydrogen is the most chemically reactive, polar hydrogen, and thus participates in oil and gas generation from coal. In contrast, non-exchangeable organic hydrogen may have preserved an isotopic paleoenvironmental signal, but

deuterium/hydrogen (D/H, or  $^2H/^1H$ ) stable isotope ratios in coals or coal kerogens are typically measured only for total hydrogen. The analytical isotopic noise from  $H_{ex}$  in total hydrogen is reduced in this study by equilibrating exchangeable organic hydrogen with isotopically characterized water vapors.

The amount of organic hydrogen in immature kerogen is insufficient to account for the total hydrogen in gas, oil, bitumen, and solid residue with increasing thermal maturity (Lewan, 1997; Schimmelmann et al., 1999). These and other studies point toward water-hydrogen as an additional source for organic hydrogen in thermally maturing organic matter, which implies that water-derived hydrogen may affect the D/H ratio of organic hydrogen in oil, gas, and coal. A better understanding of the isotopic composition and exchangeability of organic hydrogen in coal should help in evaluating the relevance of D/H ratios for paleoenvironmental reconstruction and in correlating between solid source material and the fluid products of maturation (gas, oil).

Limited data are available on the exchangeability of hydrogen in coals. Studies on the uptake of tritium ( $^3H$ ) in bulk coal in contact with tritiated water at 50–400 °C in the laboratory (Ishihara et al., 1993; Qian et al., 1997)

\* Corresponding author. Tel.: +1-604-228-2449; fax: +1-812-855-2862.

E-mail addresses: mmastale@Indiana.edu (M. Mastalerz), aschimme@indiana.edu (A. Schimmelmann).

yielded (i) an initial trend of decreasing exchangeability with increasing temperature, and (ii) a reversed trend at higher temperature, but in the presence of inorganic hydrogen in mineral-containing bulk coal these results can only be suggestive with regard to the exchangeability of organic hydrogen in coal. Particle size has little effect on  $H_{ex}$  in coal, which suggests that water-derived hydrogen has easy access via micropores and fractures (Ishihara et al., 2000; Schimmelmann et al., 2001).

This study provides  $H_{ex}$  and D/H data for mineral-free kerogen from coals and their macerals with increasing rank, and demonstrates the influence of different maceral compositions.

## 2. Techniques

A suite of Pennsylvanian coals ranging in vitrinite reflectance ( $R_o$ ) from 0.55 to 5.15% was initially selected for this study (Mastalerz and Schimmelmann, 2001). In addition, Triassic anthracite from Vietnam, Precambrian shungite from Karelia, natural graphite from British Columbia, and Miocene lignites from Poland were added to extend the range of thermal maturity. Vitrinite fractions from coals with reflectance below 1.25% were hand-picked and analyzed in addition to their respective bulk coals. A fusinite fraction from sample FGT-6 221 was hand-picked. 'Indiana paper coal' represents a coalified Pennsylvanian natural deciduous leaf assemblage (liptinite).

The ash content and elemental (ultimate) analyses of coals follow the ASTM method (1995). Vitrinite reflectance (random for coals with reflectance below 1.28%, and  $R_{max}$  for higher rank coals) and petrographic analyses were performed using a Leitz MPV-II microscope.

Prior to all isotopic analyses, mineral matter from coals and macerals was removed to yield kerogens. Our standardized kerogen preparation method employing mineral acids and heavy liquid separation, isotopic analytical procedures, and the reporting of  $H_{ex}$  in % and of  $\delta D_n$  values expressing D/H ratios of non-exchangeable organic hydrogen in customary  $\delta$ -notation followed the description given in Schimmelmann et al. (1999). The precision is  $\pm 3\text{‰}$  for  $\delta D$ ,  $\pm 0.05\text{‰}$  for  $\delta^{13}C$ , and  $\pm 0.5\%$  for  $H_{ex}$  values.

Split aliquots of kerogens were analyzed using Fourier-transform infra-red spectroscopy (FTIR). Samples for FTIR analyses were prepared using the potassium bromide (KBr) pellet method. Pellets were analyzed on a Nicolet 20SXC spectrometer equipped with a DTGS detector collecting 1024 scans per sample at a resolution of  $4\text{ cm}^{-1}$ . Bands were identified by comparison with published assignments (for example, Painter et al., 1981; Wang and Griffith, 1985; Sobkowiak and Painter, 1992).

## 3. Results

### 3.1. Coal characteristics

The majority of coals used in this study are Pennsylvanian in age and derive from the Illinois Basin (Indiana paper coal, FGT-6 221, and FGT-6 460.65, Table 1) and the Appalachian Basin (Elk Run, Herndon, Bolt, Ammonate, Baylor, and Anthracite P). Additional samples are from Vietnam (Triassic 'anthracite V'), Poland (Pennsylvanian 'anthracite LS', and Miocene lignites 2A and 14/96) and Russia (Pennsylvanian 'anthracite D'; Precambrian 'shungite B' and 'shungite D'). 'Graphite BC' is from British Columbia. These samples were selected to give a large range of coal rank, from lignite to graphite.

The ash yields of these bulk coals vary from below 1% (wt.%, dry basis) in anthracite V to more than 16% in FGT-6 221 (Table 1). H, C, N, S, and O contents from elemental (ultimate) analyses are listed in Table 1. The S content was below 1%, except for two Illinois Basin samples (FGT-6 221 and FGT-6 460.65). C and O contents in vitrinites are plotted against  $R_o$  in Fig. 1 and demonstrate well established trends of these elements with rank (Teichmüller and Teichmüller, 1979; Given, 1984; Van Krevelen, 1993).  $R_o$  ranges from around 0.2% in lignite to around 15% in graphite, thus covering coal ranks from high, medium, and low volatile bituminous, to anthracite, and meta-anthracite (Teichmüller, 1987). Reflectance of the graphite sample was not measured and is assumed to be around 15%, a value typical of well crystalline graphite (Kwiecinska, 1980).

### 3.2. Petrographic composition of coals

The petrographic composition of coals varies with rank. The two lignite samples consist almost exclusively of huminite (precursor of vitrinite), with traces of inertinite and mineral matter (Fig. 2). Although both lignites derive from vertical trunks of Miocene trees in the Bełchatów lignite deposit, Poland, they differ substantially with respect to humodetrinite and humocollinite maceral contribution (Drobnik, 2001). Coals with  $R_o$  of 0.55, 0.59, 0.88, and 0.92% show vitrinite contents between 70 and 80%, and variable amounts of liptinite and inertinite. Coals with  $R_o$  of 1.15% and higher do not contain liptinite macerals, and the amount of inertinite decreases relatively to coals with  $R_o$  of 0.55–0.92%.

### 3.3. Functional groups in coals

Lignite samples 14/19 and 2A stand out with respect to their abundances of chemical functional groups (Fig. 3). Sample 14/19 represents a very low gelification level and shows a much higher contribution of hydroxyl

groups ( $3488\text{ cm}^{-1}$ ) than the more gelified sample 2A. Sample 14/19 also shows more pronounced aliphatic stretching bands ( $2800\text{--}3000\text{ cm}^{-1}$  region) and numerous bands likely representing cellulose-derived material (e.g., at  $1512\text{ cm}^{-1}$ ) that disappear during gelification towards 2A. In fact, the FTIR spectrum of the highly gelified lignite 2A shows more similarity to the spectrum of the high volatile bituminous coal FGT-6221 with  $R_o$  0.55% (Fig. 4) than to lignite 14/96 (Fig. 3).

FTIR spectra of kerogens from vitrinite fractions of coals with  $R_o$  of 0.55 and 0.59% show minimal aromatic stretching modes ( $3000\text{--}3100\text{ cm}^{-1}$ ) and low intensity out-of-plane aromatic bands ( $700\text{--}900\text{ cm}^{-1}$ ) (Fig. 4). These aromatic bands intensify with increasing rank in coals with  $R_o$  of 1.15–3.04% (Figs. 4 and 5). The aliphatic stretching region ( $2800\text{--}3000\text{ cm}^{-1}$ ) is well developed in all coals up to  $R_o$  1.56%. Aliphatic and aromatic stretching bands are less developed in anthra-

cites (Fig. 5) and thus are unreliable proxies for aromaticity at high maturity.

The relationship between  $R_o$  and a ratio of integrated areas of aromatic stretching bands ( $3000\text{--}3100\text{ cm}^{-1}$ ) and aliphatic stretching bands ( $2800\text{--}3000\text{ cm}^{-1}$ ) for coals of high volatile bituminous rank is shown in Fig. 6. Anthracites are excluded from this graph because their respective FTIR signals are weak. The aromatic/aliphatic signal ratio is useful as a proxy for aromaticity, and the relationship in Fig. 6 shows its direct correlation ( $R^2=0.96$ ) with  $R_o$ . A comparison of these two plotted parameters from whole coal samples and their respective vitrinite fractions demonstrates that vitrinite fractions within  $R_o$  of 0.5% to about 0.9% feature slightly lower aromaticity than the bulk coal samples. For coal with  $R_o$  of 1.15 and 1.28%, the Ar/Al ratios for vitrinites and whole coal are either identical (for sample of  $R_o$  1.15%) or very close (for sample of  $R_o$  1.28%).

Table 1

Vitrinite reflectance ( $R_o$ ), hydrogen exchangeability ( $H_{ex}$ ), and H and C stable isotope ratios of kerogens from coals

| Sample        | Age System     | Region         | $R_o$ (%) | Ash dry | H daf | C daf | N daf | S dry | O daf | $H_{ex}$ (%) | $\delta D_n$ (‰) | $\delta^{13}C$ (‰) |
|---------------|----------------|----------------|-----------|---------|-------|-------|-------|-------|-------|--------------|------------------|--------------------|
| Graphite BC   | J?             | BC, Canada     | 15.00     | nd      | nd    | nd    | nd    | nd    | nd    | 13.1         | −141.4           | −14.09             |
| Shungite B    | MP             | Russia         | 7.70      | nd      | 0.6   | 97.5  | 0.8   | 0.3   | 0.8   | 5.7          | −108.4           | −37.25             |
| Shungite D    | MP             | Russia         | 6.50      | nd      | 0.5   | 97.3  | 0.7   | 0.4   | 1.1   | 3.8          | −92.4            | −29.75             |
| Anthracite D  | C              | Russia         | 5.70      | nd      | nd    | nd    | nd    | nd    | nd    | 2.3          | −88.2            | −24.06             |
| Anthracite LS | C              | Poland         | 5.10      | nd      | nd    | nd    | nd    | nd    | nd    | 2.3          | −89.0            | −22.87             |
| Anthracite P  | C              | Appalachian    | 5.15      | 2.6     | 2.01  | 94.65 | 0.91  | 0.41  | 1.30  | 3.0          | −71.9            | −23.49             |
| Anthracite V  | T              | Vietnam        | 3.04      | 0.8     | 3.42  | 94.77 | 1.39  | 0.44  | 1.28  | 2.9          | −94.3            | −24.29             |
| Baylor 13–1   | C              | Appalachian    | 1.70      | 5.6     | 3.10  | 92.35 | 1.50  | 0.45  | 2.60  | 2.2          | −91.7            | −23.33             |
| Baylor 10–2   | C              | Appalachian    | 1.56      | 5.3     | 4.89  | 89.46 | 1.55  | 0.80  | 2.87  | 3.1          | −97.0            | −23.55             |
| Ammonate      | C              | Appalachian    | 1.28      |         |       |       |       |       |       |              |                  |                    |
| Vitrinite     |                |                |           | 1.9     | 5.24  | 91.36 | 1.67  | 0.60  | 1.13  | 2.9          | −108.7           | −23.86             |
| Whole coal    |                |                |           | 11.6    | 5.24  | 89.85 | 1.53  | 0.72  | 2.66  | 2.6          | −107.2           | −23.9              |
| Bolt          | C              | Appalachian    | 1.15      |         |       |       |       |       |       |              |                  |                    |
| Vitrinite     |                |                |           | 1.3     | 5.05  | 90.97 | 1.47  | 0.54  | 1.98  | 2.8          | −97.2            | −24.24             |
| Whole coal    |                |                |           | 2.5     | 5.28  | 90.92 | 1.73  | 0.53  | 1.53  | 4.4          | −94.6            | −24.01             |
| Herndon       | C              | Appalachian    | 0.92      |         |       |       |       |       |       |              |                  |                    |
| Vitrinite     |                |                |           | 5.9     | 5.80  | 86.77 | 1.74  | 0.84  | 4.85  | 8.3          | −91.8            | −23.16             |
| Whole coal    |                |                |           | 3.7     | 5.70  | 87.29 | 1.75  | 0.75  | 4.51  | 5.3          | −94.6            | −23.63             |
| Elk Run       | C              | Appalachian    | 0.88      |         |       |       |       |       |       |              |                  |                    |
| Vitrinite     |                |                |           | 1.2     | 5.54  | 86.82 | 1.83  | 0.68  | 5.13  | 6.3          | −89.5            | −23.92             |
| Whole coal    |                |                |           | 2.4     | 5.45  | 86.90 | 1.65  | 0.65  | 5.36  | 5.3          | −91.3            | −23.64             |
| FGT-6 460.65  | C              | Illinois Basin | 0.59      |         |       |       |       |       |       |              |                  |                    |
| Vitrinite     |                |                |           | 6.1     | 5.52  | 80.94 | 1.86  | 3.44  | 8.24  | 9.7          | −83.5            | −24.29             |
| Whole coal    |                |                |           | 9.6     | 5.77  | 80.27 | 1.88  | 4.34  | 7.74  | 8.8          | −87.8            | −24.44             |
| FGT-6 221     | C              | Illinois Basin | 0.55      |         |       |       |       |       |       |              |                  |                    |
| Vitrinite     |                |                |           | 9.2     | 5.60  | 80.98 | 1.69  | 4.88  | 6.85  | 8.7          | −88.3            | −24.01             |
| Fusain        |                |                |           | 20.1    | 3.88  | 82.12 | 1.00  | 7.85  | 5.15  | 5.1          | −72.6            | −23.85             |
| Whole coal    |                |                |           | 16.4    | 5.71  | 79.87 | 1.66  | 2.88  | 9.87  | 9.0          | −90.1            | −24.38             |
| Indiana paper | C              | Illinois Basin | 0.54      |         |       |       |       |       |       | 6.3          | −84.2            | −24.4              |
| Lignite 2A    | N <sub>1</sub> | Poland         | 0.23      | 2.4     | 5.56  | 67.70 | 0.42  | 0.70  | 25.50 | 18.6         | −135.0           | −23.1              |
| Lignite 14/96 | N <sub>1</sub> | Poland         | 0.16      | 1.4     | 6.4   | 57.90 | 0.13  | 0.17  | 35.37 | 17.2         | −87.0            | −23.2              |

MP, Mesoproterozoic; C, Pennsylvanian; T, Triassic; J, Jurassic; N<sub>1</sub>, Miocene; nd, not determined.

Elemental (ultimate) analyses utilized bulk coal, with reported values (wt.%) calculated on dry ash-free basis, with the exception of S.

### 3.4. Hydrogen in coals

The relative abundance of  $H_{ex}$  is highest in lignite with about 18% of total hydrogen and with rising maturity decreases to around 2.5% in coals with  $R_o$  of

ca. 1.7 to ca. 5.7% (Table 1, Fig. 7A). The two data points in Fig. 7 with  $R_o > 6\%$  suggest a late rise in  $H_{ex}$  with increasing maturity, in spite of the fact that the abundance of total organic hydrogen decreases (Table 1). The relationship between  $H_{ex}$  and total

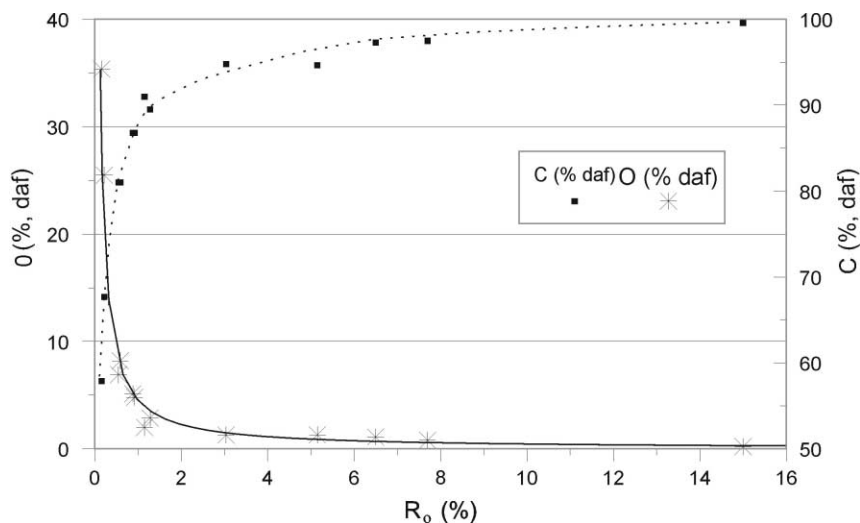


Fig. 1. Carbon and oxygen contents of coals, via elemental (ultimate) analysis, calculated for dry ash-free organic matter. Lines are drawn to indicate trends and to guide the eye.

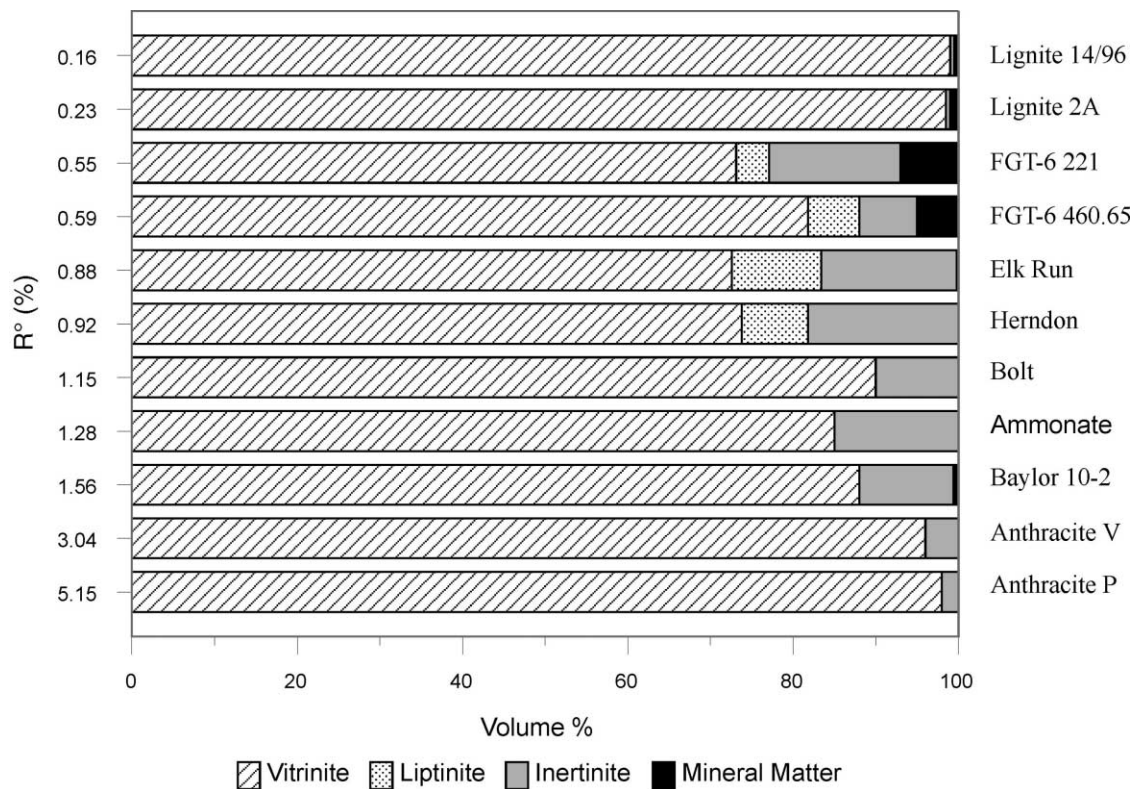


Fig. 2. Maceral composition of the coals.  $R_o$ —vitrinite reflectance.

organic hydrogen (dry wt.%) in kerogen is shown in Fig. 7B. The close similarity to Fig. 7A is based on the fact that the hydrogen content in coals is related to thermal rank. Thermally immature coals with much organic hydrogen also feature initially high  $H_{\text{ex}}$ . Both parameters decline with increasing rank, with  $H_{\text{ex}}$  quickly dropping at an accelerated pace and then staying level between  $R_o$  of 2–6%. At a more mature rank,  $H_{\text{ex}}$  shows an increase (up to 13.1% in graphite) while the hydrogen abundance continues its approach to a value of zero for ideal graphite.

Comparative data show that  $H_{\text{ex}}$  of kerogen from bulk coal tends to be smaller than  $H_{\text{ex}}$  of the vitrinite kerogen from the same coal (Fig. 8A), although the analytical precision of  $H_{\text{ex}}$  values of  $\pm 0.5\%$  renders many comparisons uncertain. Fusinite from coal FGT-6 221 shows a reduced  $H_{\text{ex}}$  of 5.1% when compared with  $H_{\text{ex}}$  of 9.0% in kerogen from the parent bulk coal (Table 1, Fig. 8B). No liptinite fraction was available from this coal, but a comparison is possible with ‘Indiana paper coal’ that derives from a sequence with the same maturity and consists almost exclusively of cutinite (Crelling and Bensley, 1980). The  $H_{\text{ex}}$  value of 6.3% for ‘Indiana paper coal’ is intermediate between values for vitrinite and fusinite (Fig. 8B).

Hydrogen isotope ratios for the non-exchangeable organic hydrogen in kerogens do not show an overall consistent trend with maturity (Fig. 9). A trend is suggested toward negative  $\delta D_n$  values for Illinois Basin and Appalachian Basin coals within a  $R_o$  range of 0.55–1.4%. In most cases,  $\delta D_n$  values of non-exchangeable H in kerogens from whole coal samples are similar to those of the respective vitrinite fractions (Fig. 9). Fusinite, on the other hand, shows a significantly less negative  $\delta D_n$  value than the vitrinite and whole coal. Indiana paper

coal features an intermediate value between vitrinite and fusinite.

### 3.5. Carbon isotope ratios

With only three exceptions, all kerogen  $\delta^{13}\text{C}$  values cluster narrowly between  $-22.87\text{‰}$  and  $-24.44\text{‰}$  (Table 1). The two Precambrian shungites are significantly more negative, a feature not uncommon for some Precambrian organic matter (Galimov, 1980; Schidlowski et al., 1983). In contrast, graphite is more  $^{13}\text{C}$ -enriched which may in part reflect a history of thermal methanogenesis that eliminated  $^{12}\text{C}$  in form of  $^{13}\text{C}$ -depleted methane (Galimov, 1980).

## 4. Discussion

### 4.1. Exchangeable organic hydrogen

Although all hydrogen in  $-\text{OH}$ ,  $-\text{COOH}$ ,  $-\text{NH}_2$ ,  $-\text{SH}$ , and other H-containing functional groups is potentially exchangeable with ambient water hydrogen, the actual exchange reaction requires access of water molecules. Kerogen molecules are typically very large, chemically complex, and may have a sterically rigid 3D-structure that prevents or restricts access of water molecules to some functional groups, similar to large aliphaticenes (Mujica et al., 2000).  $H_{\text{ex}}$  is therefore not an absolute measure for the abundance of hydrogen-containing functional groups in kerogen, but is operationally defined in this study to reflect isotopic exchangeability at 115 °C over 8 h. Nevertheless,  $H_{\text{ex}}$  is a proxy for the chemical accessibility, and thus relates to the reactivity, of H-containing functional groups in kerogen macromolecules.

Exchangeable hydrogen accounts for 2.3–18.6% of total hydrogen in kerogens from coals (Table 1, Fig. 7A), with the highest values (18.6 and 17.2%) recorded for thermally immature Miocene lignite samples. Cellulose with  $H_{\text{ex}}$  above 20% (Schimmelmann et al., 1993) is a likely major contributor to the original precursor biomass of lignites.

$H_{\text{ex}}$  shows some variability among coals of comparable thermal maturity, and even more between pure vitrinite fractions of these coals. The lignin-rich (phenolic) source material of vitrinite seems to be the reason that all vitrinite kerogens exhibit higher  $H_{\text{ex}}$  than kerogens from the respective bulk coals (except FGT221; Fig. 8A), with the largest difference for coals having reflectance values of  $R_o$  0.92% (Herndon) and 1.15% (Bolt). No vitrinite fraction was available from coal with  $R_o$  1.56% (Baylor). Homogenization of maceral properties in anthracites did not permit a separation of vitrinites. The  $H_{\text{ex}}$  of fusinite kerogen from coal FGT-6 221 is much lower than  $H_{\text{ex}}$  in kerogens from the

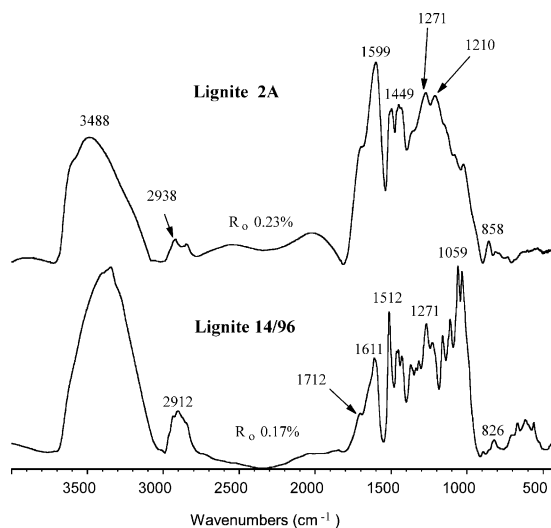


Fig. 3. FTIR spectra of lignite samples.

accompanying vitrinite or parent coal, suggesting that charring of wood during wildfires reduces  $H_{ex}$ . A significant contribution of fusinite or inertinite should thus decrease  $H_{ex}$  in bulk coal kerogen. The coal with the

highest inertinite content (about 20% in Herndon coal with  $R_o$  0.92%; Fig. 2) indeed shows relatively low  $H_{ex}$  regardless of the high  $H_{ex}$  of its vitrinite fraction. At a rank equivalent to  $R_o$  1.28% and higher, differences in

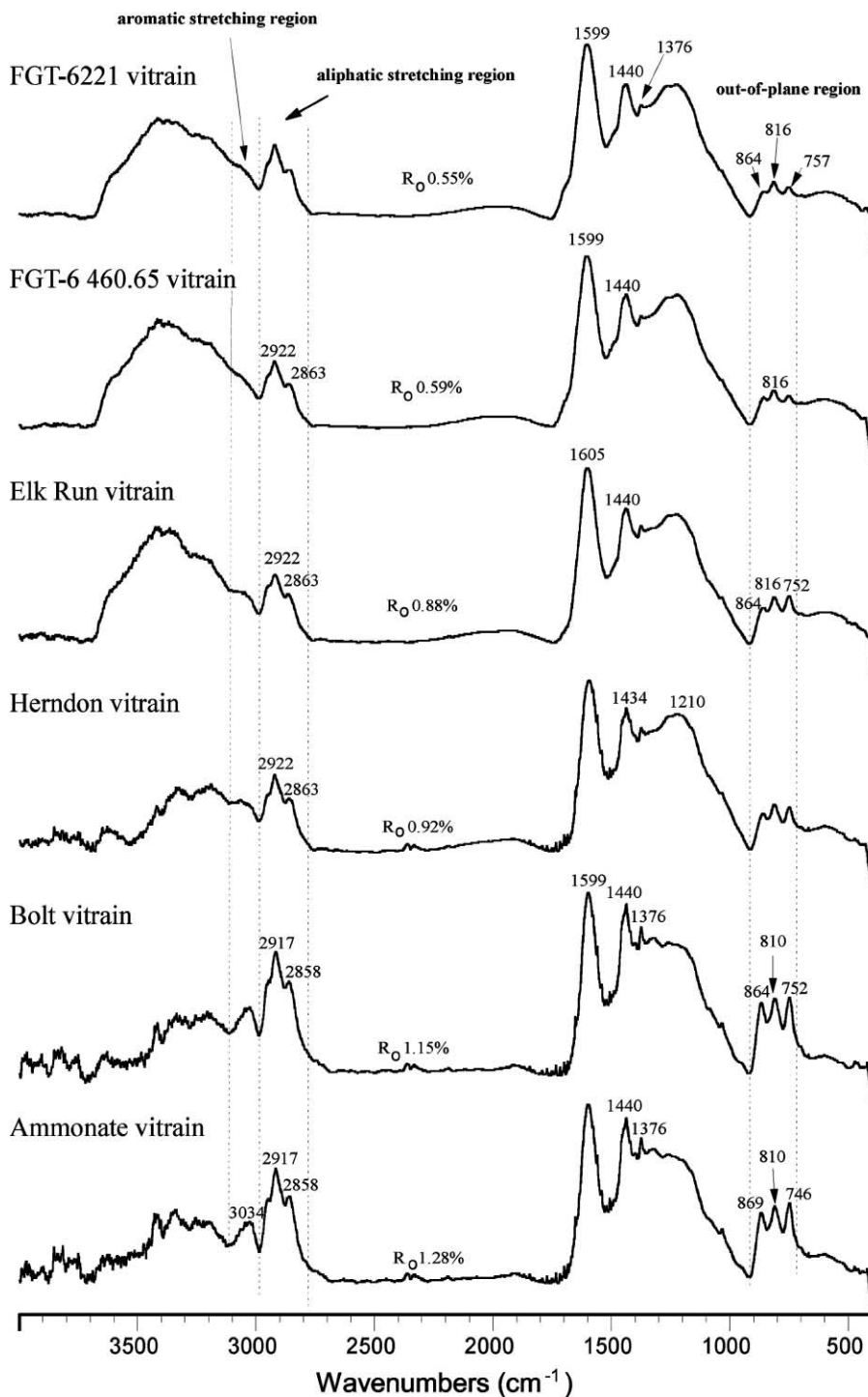


Fig. 4. FTIR spectra of bituminous coals.

$H_{\text{ex}}$  between maceral types diminish greatly. Consequently, if the abundance of exchangeable hydrogen influences the gas potential of coals, the maceral composition will be a decisive factor up to high volatile bituminous rank, but will have lost much importance at higher ranks.

The influence of liptinite macerals on  $H_{\text{ex}}$  is unclear. Cutinite from Indiana paper coal shows a transitional value between fusinite and vitrinite of the same rank coal (Fig. 8B). However, the sample has been weathered and its  $H_{\text{ex}}$  value may be diagenetically lowered relative to unweathered cutinite. Liptinite macerals usually contain more hydrogen than associated vitrinite (Mastalerz and Bustin, 1993). If vitrinite and liptinite follow the same principle as vitrinite and fusinite (e.g., larger  $H_{\text{ex}}$  for more H within bituminous rank, Fig. 7B), larger  $H_{\text{ex}}$  would be expected from liptinite macerals. Additional data on fresh liptinite macerals are needed.

A dramatic reduction of  $H_{\text{ex}}$  occurs via thermal elimination of chemical functional groups (e.g.,  $-\text{OH}$ ,  $-\text{COOH}$ , etc.) and a relative increase in the abundance of aromatic  $\equiv\text{CH}$  at the expense of aliphatic  $=\text{CH}_2$  in coals during the transition from  $R_o$  0.16 to 1.15% (Figs. 3, 4, 7A). Increased aromaticity of kerogens at higher maturity provides for increased relative abundances of aromatic carbon-bound H with low  $pK_a$  (proton acidity). This aromatic exchangeable hydrogen (Alexander et al., 1981; 1982; Long et al., 1981; Werstiuk and Ju, 1989) partially compensates for the loss of

exchangeable hydrogen from thermally eliminated functional groups.

An isotopic implication of the presence of exchangeable hydrogen in coal for hydrocarbon generation is the transfer of ambient hydrogen (e.g., inorganic hydrogen from formation waters, or organic hydrogen in hydrocarbons, etc.) to organic exchangeable hydrogen in kerogen, providing a mechanism for the isotopic signature of formation waters (Polya et al., 2000) and other hydrogen pools to influence bulk  $\delta\text{D}$  values of kerogen and its maturation products. Chemical maturation reactions involving organic hydrogen are not restricted to isotopically exchangeable hydrogen. Based on hydrous pyrolysis experiments (Lewan, 1997; Schimmelmann et al., 1999), it has been argued that water plays an important role in hydrocarbon generation from source rocks, an idea also expressed earlier by numerous researchers (Jurg and Eisma, 1964; Hesp and Rigby, 1973; Lewan et al., 1979; Hoering, 1984; Stalker et al., 1998). According to Lewan (1997), utilization of inorganic H from formation waters promotes cracking and at the same time retards the thermal destruction of hydrocarbons by quenching free radical sites before they participate in organic cross-linking reactions. This, in turn, extends the thermal stability of hydrocarbons. The same considerations are likely important for natural gas generation from coal, where water is present in substantial quantities. Several thermolytic and catalytic pathways were suggested to operate in coal, depending on rank, chemical composition, and the availability of catalysts (Butala et al., 2000).

#### 4.2. Non-exchangeable organic hydrogen

The isotopically non-exchangeable portion of organic H is chemically more stable than exchangeable H, and  $\delta\text{D}_n$  values of non-exchangeable H may therefore

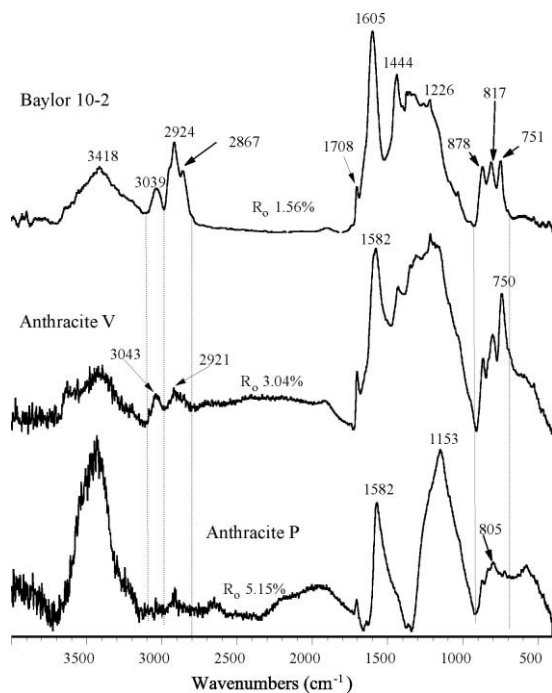


Fig. 5. FTIR spectra of Baylor coal and anthracites.

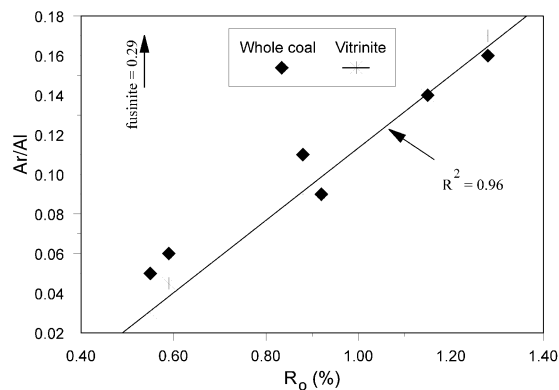


Fig. 6. Relationship between the ratio of integrated areas of the aromatic stretching bands (region 3000–3100  $\text{cm}^{-1}$ ) to aliphatic stretching bands (region 2800–3000  $\text{cm}^{-1}$ ) and vitrinite reflectance ( $R_o$ ). A linear regression is fitted to the vitrinite data.

provide information about the depositional paleoenvironment (Smith et al., 1982, 1983; Krishnamurthy et al., 1995; Schimmelmann et al., 2000). Not only did the paleoenvironments of our samples differ greatly, but diagenetic changes in  $\delta D_n$  values of non-exchangeable organic hydrogen via thermal maturation reactions are likely (Schimmelmann et al., 1999, 2000), thus explaining the apparent lack of overall correlation between  $\delta D_n$  and reflectance values in this study (Fig. 9).

Two isotopic comparisons between specific samples are warranted. The two low-maturity lignite samples 2A

and 14/96 were deposited  $\sim 18$  Ma ago in a warm temperate climate at  $\sim 50^\circ \text{N}$  (Burchart et al., 1988). They show surprisingly different  $\delta D_n$  values (Fig. 9), although both samples derive from the same Polish coal mine and represent the same Miocene tree species. Sample 2A is more gelified and likely contains less cellulose-derived organic matter than sample 14/96. It may be of importance that the horizons of the two fossil tree trunks are separated by a volcanic-derived tonstein layer that is a few centimeters thick. We speculate that geomorphological changes in the wake of the volcanic eruption

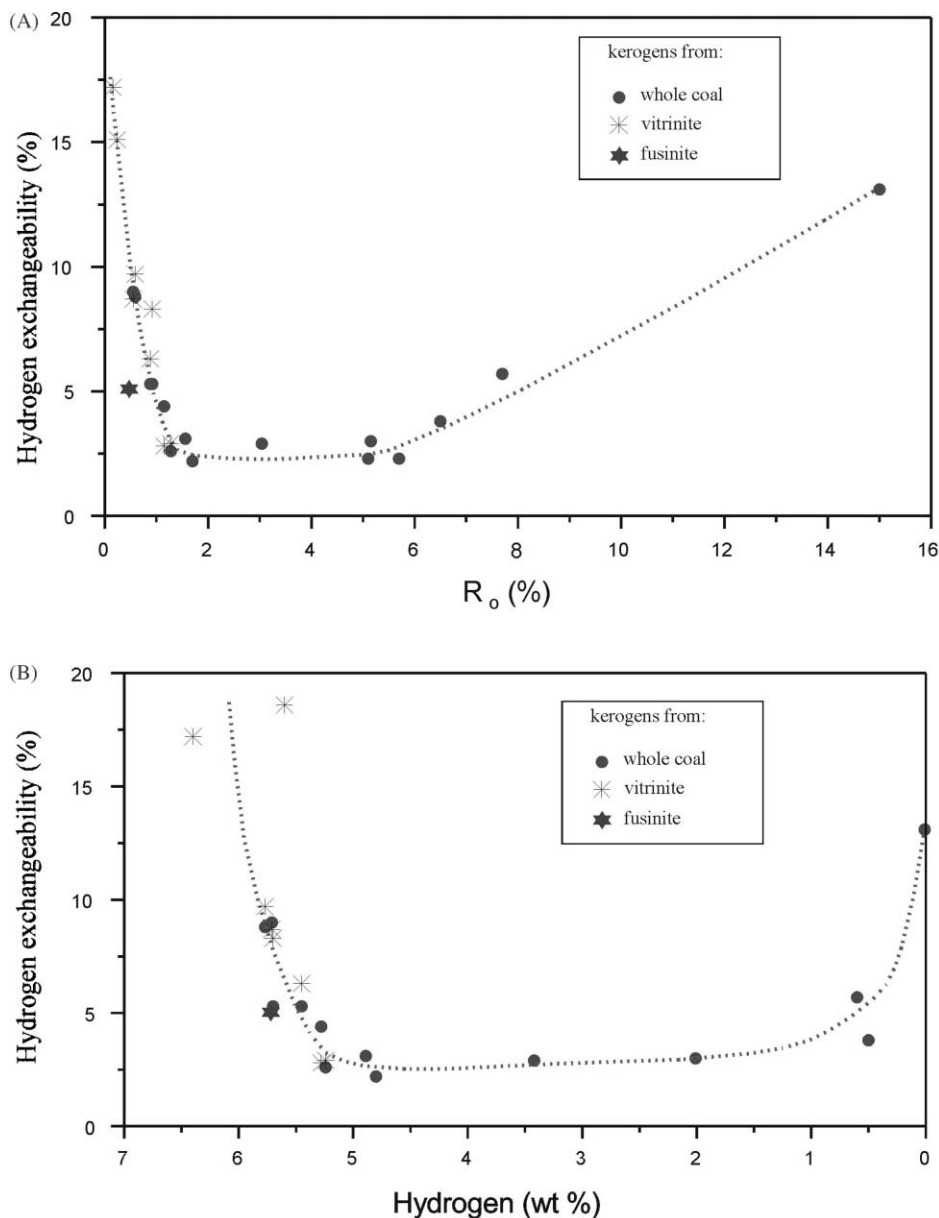


Fig. 7. (A) Relationship between hydrogen exchangeability ( $H_{ex}$ ) and vitrinite reflectance ( $R_o$ ). (B) Relationship between  $H_{ex}$  and total H content. Line is drawn to indicate trends and to guide the eye.



caused changes in the local hydrology and the isotopic signature of the water source available for tree growth.

The second comparison focuses on coals from the Illinois Basin and Appalachian Basin. This group shifts towards more negative  $\delta D_n$  values with increasing maturity (Fig. 9). The Pennsylvanian coals from both basins were deposited geographically close to one another ( $\sim 5^\circ$  S) in similar tropical climates (Scotese, 1994). The isotopic trend suggests that maturation

either preferentially eliminated deuterium  $^2H$  and/or preferentially added  $^1H$  to kerogen. Organic H linked to oxygen and nitrogen tends to be more enriched in deuterium than carbon-linked organic hydrogen (Schimmelmann et al., 1999). Some of this  $^2H$  in functional groups is sterically inaccessible to water during isotopic equilibration and thus contributes to the pool of non-exchangeable hydrogen. We hypothesize that thermal maturation eliminates some  $^2H$ -enriched functional groups, thus accounting for the observed shift towards

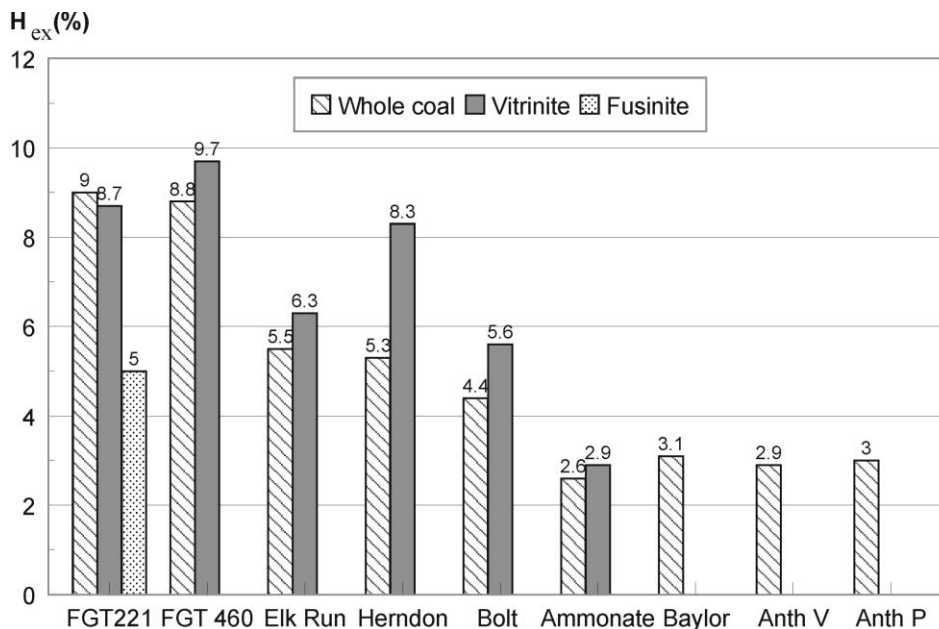


Fig. 8. (A) Hydrogen exchangeability  $H_{ex}$  in kerogens from whole coal and vitrinite fractions for individual coal samples.  $H_{ex}$  for fusinite was determined for sample FGT221.

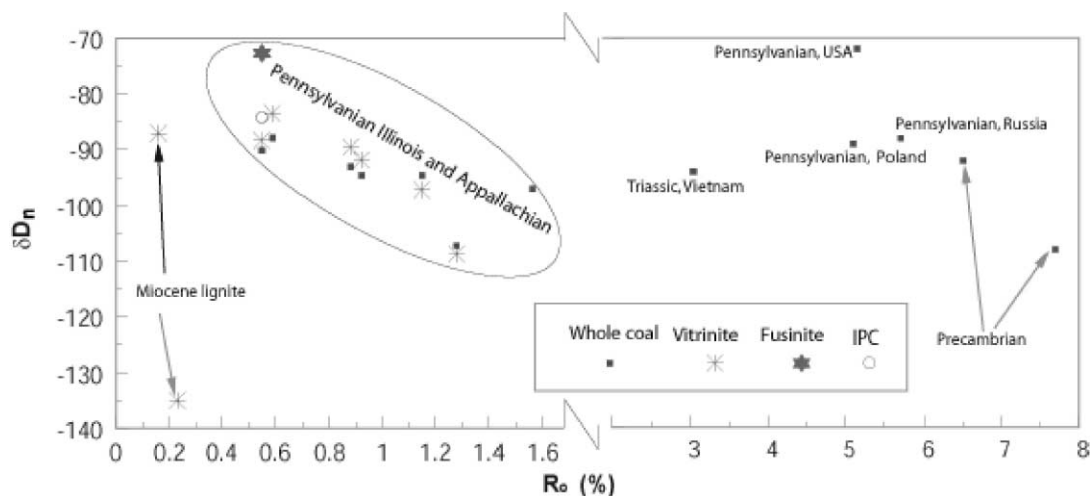


Fig. 9.  $\delta D_n$  values of non-exchangeable organic hydrogen in kerogens from the coals studied.

more negative  $\delta D_n$ . An alternative explanation, namely addition of water-derived  $^1H$  to organic hydrogen, is possible when thermally maturing kerogen is in contact with  $^2H$ -depleted formation waters that derive from mid- to high-latitude precipitation. Coals of tropical origin would need to have their pore waters exchanged before coalification. There is no paleogeographic evidence that the coals in question were ever in contact with strongly  $^2H$ -depleted meteoric waters before they reached the present level of maturation.

For the higher rank kerogens with  $R_o > 3$  (Fig. 9) we observe no statistically significant isotopic trend with maturation. The isotopic similarity of Carboniferous coals from Russia and Poland and the Triassic coal from Vietnam may reflect their common tropical origin, within a few degrees of the equator (Fig. 9).

## 5. Conclusions

- Exchangeable hydrogen accounts for 2.3–18.6% of total hydrogen in kerogens from coals (Table 1, Fig. 7A), with the highest values (18.6 and 17.2%) recorded for lignite. Its abundance depends primarily on coal rank. The maceral composition influences  $H_{ex}$  up to the rank of high volatile bituminous coal and becomes irrelevant at higher ranks.
- Quantification of hydrogen isotopic exchangeability in kerogen from bulk coal and in isolated macerals offers an analytically independent proxy for assessing organic-geochemical processes during thermal maturation.
- Directly measured hydrogen stable isotope ratios of bulk coal, even after careful demineralization, reflect (1) the maceral composition and original isotopic signals from biomass, (2) the history of coal-water isotopic interaction during thermal maturation of organic matter, and (3) the presence of isotopically exchangeable organic hydrogen. The latter complication can be mitigated by isotopic double-equilibration of exchangeable hydrogen, thus arriving at the isotopic composition of non-exchangeable organic hydrogen.

## Acknowledgements

This work was supported by Department of Energy Basic Energy Research Grant number DE-FG02-00ER15032. We thank A.E. Fallick and G.D. Love for their constructive reviews and suggestions.

Associate Editor—C. Snape

## References

- Alexander, R., Kagi, R.I., Larcher, A.V., Woodhouse, G.W., 1981. Aromatic hydrogen exchange in petroleum source rocks. In: Bjorøy, M. et al. (Eds.), *Advances in Organic Geochemistry 1981*. Chichester, Wiley, pp. 69–71.
- Alexander, R., Kagi, R.I., Larcher, A.V., 1982. Clay catalysis of aromatic hydrogen-exchange reactions. *Geochimica et Cosmochimica Acta* 46, 219–222.
- ASTM, 1995. *Annual Book of American Society for Testing and Materials Standards*. Sec. 05.05 Gaseous Fuels; Coal and Coke. American Society for Testing and Materials, Philadelphia, PA.
- Burchart, J., Kasza, L., Lorenc, S., 1988. Fission-track zircon dating of tuffitic intercalations (tonstein) in the brown-coal mine “Belchatów”. *Bulletin of the Polish Academy of Sciences* 36, 281–286.
- Butala, S.J.M., Medina, J.C., Taylor, T.Q., Bartholomew, C.H., Lee, M.L., 2000. Mechanisms and kinetics of reactions leading to natural gas formation during coal maturation. *Energy and Fuels* 14, 235–259.
- Crelling, J.C., Bensley, D.F., 1980. Petrology of cutinite-rich coal from the Roaring Creek Mine area, Parke County, Indiana. Tenth Annual Field Conference, Great Lake Section, Society of Economic Paleontologists and Mineralogists, Danville, 26–28 September, 1980, pp. 93–105.
- Drobniak, A., 2001. Proces zelifikacji ksyliotów w świetle badań paleobotaniczno-petrograficznych i chemicznych na przykładzie złoża węgla brunatnego “Belchatów”. Unpublished PhD dissertation, Akademia Gorniczo-Hutnicza, Kraków (in Polish).
- Galimov, E.M., 1980.  $C^{13}/C^{12}$  in kerogen. In: Durand, B. (Ed.), *Kerogen*. Editions Technip, Paris, pp. 271–298.
- Given, P.H., 1984. An essay on the organic geochemistry of coal. *Coal Science* 3, 63–252.
- Hesp, W., Rigby, D., 1973. The geochemical alteration of hydrocarbons in the presence of water. *Erdöl & Kohle, Erdgas, Petrochemie* 26, 70–76.
- Hoering, T.C., 1984. Thermal reactions of kerogen with added water, heavy water, and pure organic substances. *Organic Geochemistry* 5, 267–278.
- Ishihara, A., Takaoka, H., Nakajima, E., Imai, Y., Kabe, T., 1993. Estimation of hydrogen mobility in coal using a tritium tracer method. Hydrogen exchange reactions of coals with tritiated water and molecular hydrogen. *Energy and Fuels* 7, 362–366.
- Ishihara, A., Nishigori, D., Saito, M., Qian, W., Kabe, T., 2000. Hydrogen exchange reactions of coal with tritiated gaseous hydrogen and water. Effects of particle size of coal on hydrogen exchange. *Energy and Fuels* 14, 706–711.
- Jurg, J.W., Eisma, E., 1964. Petroleum hydrocarbons: generation from fatty acids. *Science* 144, 1451–1452.
- Krishnamurthy, R.V., Syrup, K.A., Baskaran, M., Long, A., 1995. Late glacial climate record of midwestern United States from the hydrogen isotope ratio of lake organic matter. *Science* 269, 1565–1567.
- Kwiecinska, B., 1980. Mineralogy of natural graphite. *Prace Mineralogiczne* 67, Polska Akademia Nauk, 1–87.
- Lewan, M.D., 1997. Experiments on the role of water in petroleum formation. *Geochimica et Cosmochimica Acta* 61, 3691–3723.

- Lewan, M.D., Winters, J.C., McDonald, J.H., 1979. Generation of oil-like pyrolyzates from organic-rich shales. *Science* 203, 897–899.
- Long, M.A., Garnett, J.L., Williams, P.G., Mole, T., 1981. Tritium labeling of organic compounds by HNaY zeolite catalyzed exchange with tritiated water and their analysis by  $^3\text{H}$  NMR. *J. Am. Chem. Soc.* 103, 1571–1572.
- Mastalerz, M., Bustin, R.M., 1993. Variation in maceral chemistry within and between coals of varying rank: an electron microprobe and micro-Fourier transform infra-red investigation. *Journal of Microscopy* 171, 153–166.
- Mastalerz, M., Schimmelmann, A., 2001. Isotopically exchangeable hydrogen in coal relates to thermal maturity and maceral composition. In: Abstracts of the TSOP/ICCP Session, The 53rd meeting of the International Committee for Coal and Organic Petrology, Copenhagen, pp. 16–19.
- Mujica, V., Nieto, P., Puerta, L., Acevedo, S., 2000. Caging of molecules by alphasenes. A model for free radical preservation in crude oils. *Energy and Fuels* 14, 632–639.
- Painter, P.C., Snyder, R.M., Starsinic, M., Coleman, M.M., Kuehn, D.W., Davis, A., 1981. Concerning the application of FTIR to the study of coal: a critical assessment of band assignments and the application of spectral analysis programs. *Applied Spectroscopy* 35, 475–485.
- Polya, D.A., Foxford, K.A., Stuart, F., Boyce, A., Fallick, A.E., 2000. Evolution and paragenetic context of low  $\delta\text{D}$  hydrothermal fluids from the Panasqueira W-Sn deposit, Portugal: new evidence from microthermometric, stable isotope, noble gas and halogen analyses of primary fluid inclusions. *Geochimica et Cosmochimica Acta* 64, 3357–3371.
- Qian, W., Ishihara, A., Fujimura, H., Saito, M., Godo, M., Kabe, T., 1997. Elucidation of hydrogen mobility in coal using a tritium tracer method. 1. Hydrogen exchange reaction of coal with tritiated water. *Energy and Fuels* 11, 1288–1292.
- Schidlowski, M., Hayes, J.M., Kaplan, I.R., 1983. Isotopic inferences of ancient biochemistries: carbon, sulfur, hydrogen, and nitrogen. In: Schopf, J.W. (Ed.), *Earth's Earliest Biosphere, Its Origin and Evolution*. Princeton University Press, Princeton, NJ, pp. 149–186. (Chapter 7).
- Schimmelmann, A., Miller, R.F., Leavitt, S.W., 1993. Hydrogen isotopic exchange and stable isotope ratios in cellulose, wood, chitin, and amino compounds. In: *Climate Change in Continental Isotopic Records*. Geophysical Monograph 78. American Geophysical Union, pp. 367–374.
- Schimmelmann, A., Lewan, M.D., Wintsch, R.P., 1999. D/H isotope ratios of kerogen, bitumen, oil, and water in hydrous pyrolysis of source rocks containing kerogen types I, II, IIS, and III. *Geochimica et Cosmochimica Acta* 63, 3751–3766.
- Schimmelmann, A., Lawrence, M., Michael, E., 2000. Stable isotope ratios of organic H, C, and N in the Miocene Monterey Formation, California. In: Isaacs, C.M., Rullkötter, J. (Eds.), *The Monterey Formation: From Rocks to Molecules*. Columbia University Press, New York, pp. 86–106.
- Schimmelmann, A., Boudou, J.-P., Lewan, M.D., Wintsch, R.P., 2001. Experimental controls on D/H and  $^{13}\text{C}/^{12}\text{C}$  ratios of kerogen, bitumen and oil during hydrous pyrolysis. *Organic Geochemistry* 31, 1009–1018.
- Scotese, C.R., 1994. Carboniferous paleocontinental reconstructions. In: Cecil, C.C., Edgar, N.T. (Eds.), *Predictive Stratigraphic Analysis; Concept and Application*. U.S. Geological Survey Bulletin, Reston, VA, pp. 3–6.
- Stalker, L., Larter, S.R., Farrimond, P., 1998. Biomarker binding into kerogens: evidence from hydrous pyrolysis using heavy water ( $\text{D}_2\text{O}$ ). *Organic Geochemistry* 28, 239–253.
- Smith, J.W., Gould, K.W., Rigby, D., 1982. The stable isotope geochemistry of Australian coals. *Organic Geochemistry* 3, 111–131.
- Smith, J.W., Rigby, D., Schmidt, Clark, D.A., 1983. D/H ratios of coals and the palaeolatitude of their deposition. *Nature* 302, 322–323.
- Sobkowiak, M., Painter, P., 1992. Determination of the aliphatic and aromatic CH contents of coals by FT-i.r. studies of coal extracts. *Fuel* 71, 1105–1125.
- Teichmüller, M., 1987. Organic matter and very low-grade metamorphism. In: Frey, M. (Ed.), *Low Temperature Metamorphism*. Blackie, Glasgow, pp. 114–161.
- Teichmüller, M., Teichmüller, R., 1979. Diagenesis of coal (coalification). In: Larsen, G., Chilingar, G.V. (Eds.), *Diagenesis in Sediments and Sedimentary Rocks*. Elsevier, Amsterdam, pp. 207–246.
- Van Krevelen, D.W., 1993. *Coal: Typology, Chemistry, Physics, Constitution*, third ed. Elsevier, Amsterdam.
- Wang, S.H., Griffith, P.R., 1985. Resolution enhancement of reflectance IR spectra of coals by Fourier-self-deconvolution. 1. C-H stretching and bending modes. *Fuel* 64, 229–236.
- Werstiuk, N.H., Ju, C., 1989. Protium-deuterium exchange of benzo-substituted heterocycles in neutral  $\text{D}_2\text{O}$  at elevated temperatures. *Can. J. Chem.* 67, 812–815.